

Evaluating Decision Optimality of Autonomous Driving via Metamorphic Testing

Mingfei Cheng
Singapore Management University
Singapore

Yuan Zhou
Nanyang Technological University
Singapore

Xiaofei Xie
Singapore Management University
Singapore

Junjie Wang
Tianjin University
China

Guozhu Meng
Chinese Academy of Sciences
China

Kairui Yang
Alibaba Group
China

ABSTRACT

Autonomous Driving System (ADS) testing is crucial in ADS development, with the current primary focus being on safety. However, the evaluation of non-safety-critical performance, particularly the ADS’s ability to make optimal decisions and produce optimal paths for autonomous vehicles (AVs), is equally vital to ensure the intelligence and reduce risks of AVs. Currently, there is little work dedicated to assessing ADSs’ optimal decision-making performance due to the lack of corresponding oracles and the difficulty in generating scenarios with non-optimal decisions. In this paper, we focus on evaluating the decision-making quality of an ADS and propose the first method for detecting non-optimal decision scenarios (NoDSs), where the ADS does not compute optimal paths for AVs. Firstly, to deal with the oracle problem, we propose a novel metamorphic relation (MR) aimed at exposing violations of optimal decisions. The MR identifies the property that the ADS should retain optimal decisions when the optimal path remains unaffected by non-invasive changes. Subsequently, we develop a new framework, *Decictor*, designed to generate NoDSs efficiently. *Decictor* comprises three main components: Non-invasive Mutation, MR Check, and Feedback. The Non-invasive Mutation ensures that the original optimal path in the mutated scenarios is not affected, while the MR Check is responsible for determining whether non-optimal decisions are made. To enhance the effectiveness of identifying NoDSs, we design a feedback metric that combines both spatial and temporal aspects of the AV’s movement. We evaluate *Decictor* on Baidu Apollo, an open-source and production-grade ADS. The experimental results validate the effectiveness of *Decictor* in detecting non-optimal decisions of ADSs. It generates 46.0 NoDSs from 4 initial scenarios, while the best-performing baseline only detects 19.7 NoDSs. Our work provides valuable and original insights into evaluating the non-safety-critical performance of ADSs.

1 INTRODUCTION

Autonomous Driving Systems (ADSs) have been a revolutionary technology with the potential to transform our transportation system into an intelligent one. ADSs aim to enable vehicles to operate without human intervention, relying on a combination of different sensors (e.g., camera, radar, lidar, and GPS) and artificial intelligence algorithms to perceive the environment, make decisions, and navigate safely. Even though the development of ADSs has seen significant progress over the past few decades, it is still a great challenge to guarantee that the ADSs can satisfy all performance

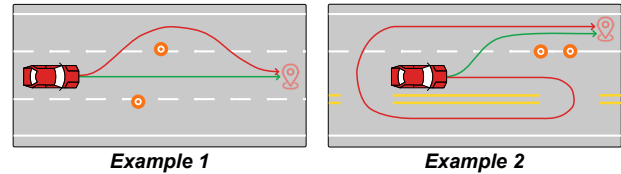


Figure 1: Examples of non-optimal decision scenarios. Green lines are expected optimal paths and Red lines are non-optimal paths generated by the ADS.

requirements under different situations due to the existing vulnerabilities in ADSs [13]. Therefore, before their real-world deployment, ADSs should be sufficiently tested [24].

Usually, the requirements of ADSs can be classified as safety-critical and non-safety-critical. Safety-critical requirements are those essential for ensuring safe operations and performance of the autonomous vehicle and the environment. For example, an ADS should guarantee that the ego vehicle (i.e., the autonomous vehicle controlled by the ADS) should arrive at its destination without causing collisions or violating traffic rules. Non-safety-critical requirements refer to aspects that do not directly impact safety performance but are important for positive user experiences and optimal vehicle performance, such as motion efficiency, passenger comfort, and energy consumption.

Currently, various testing technologies have been proposed to evaluate the safety-critical requirements of ADSs (referred to as “safety testing”), such as data-driven methods [4, 8, 28, 40] and guided searching methods [1, 6, 12, 16, 18, 23, 42]. They aim to generate safety-critical scenarios, under which the ego vehicle will cause safety issues, such as collisions and traffic rule violations. Some ADS testing works [20, 25] consider simple non-safety-critical requirements, such as comfort measured by acceleration. However, to the best of our knowledge, there is scant research on evaluating the decision optimality of ADSs (referred to as “optimal decision testing”). This aspect is an important non-safety-critical requirement and is crucial in generating optimal paths and guaranteeing motion efficiency for the ego vehicle in complex traffic scenarios. This type of testing aims to explore scenarios where safety risks are not present but remain crucial for assessing the overall intelligence and decision quality of the ADS.

Figure 1 showcases two examples of non-safety-critical violations where the ADS does not generate optimal paths. Note that these violations are not safety violations, as they still enable the ego vehicle to reach its destination safely. An intelligent ADS is expected to accurately appraise the traffic conditions and select

the most efficient path to reach its destination. However, a less intelligent ADS may fall short in accurately interpreting traffic situations and make non-optimal decisions, resulting in non-optimal paths. It might unnecessarily hold back for an extended period despite a clear intersection or choose an inefficient path, leading to unnecessary delays or safety risks. Hence, assessing the quality of decision-making in ADSs is of significant importance. Non-optimal decisions can impact the overall comfort, efficiency, and energy consumption of autonomous vehicles and may even introduce potential safety risks.

In this paper, we present the first dedicated study on optimal decision testing for ADSs, focusing specifically on the detection of *non-optimal decisions*, i.e., those completing motion tasks safely with non-optimal paths. However, testing decision optimality and identifying corresponding violations pose unique challenges: (1) One challenge arises from the lack of explicit test oracles in optimal decision testing. Safety-critical violations and simple non-safety-critical violations (i.e., comfort) can be easily identified using clear and quantified criteria. For example, comfort can be assessed through abnormal acceleration. However, in optimal decision testing, no such oracles exist for evaluating the optimality of the paths made by the ADS. Determining whether the ADS has selected an optimal path or made the best decisions to reach the destination in a scenario becomes challenging. (2) Another challenge emerges due to the infinite and unpredictable nature of road conditions [16, 42]. Road scenarios featuring variable road users and environmental factors create an infinite scenario space, complicating the generation of scenarios that violate the optimal decision requirement, referred to “**Non-optimal Decision Scenarios**” (NoDSs). Consequently, efficiently identifying NoDSs becomes a crucial challenge.

To address these challenges, we introduce a novel metamorphic testing method called *Decictor*. This method effectively and efficiently detects violations of optimal decisions and the corresponding NoDSs. ❶ To tackle the first challenge, we propose a metamorphic relation (MR) that is designed to expose scenarios with non-optimal paths. The MR is defined as: the ADS should consistently make optimal decisions within a scenario, even after undergoing certain non-invasive changes that do not affect the original driving path. The violation of the MR indicates that the ADS is not making optimal decisions. ❷ To tackle the second challenge with regards to effectively detecting NoDSs, we propose a search-based testing method comprising three main components: *Non-invasive Mutation*, *MR Check*, and *Feedback*. Given an “**Optimal Decision Scenario**” (ODS) where the ADS produces an optimal path, *Decictor* employs non-invasive mutation to modify the behaviors of other participants, which does not affect the original optimal path taken by the ego vehicle. After the mutation, an abstraction-based behavior comparison is performed to check the validity of the MR. This step involves comparing the ego vehicle’s driving paths between the ODS and the mutated scenario. If the driving paths are different in the two scenarios, it suggests that the ADS has deviated from making optimal decisions. To provide feedback about the deviations that guide the generation of NoDSs, *Decictor* introduces a novel fitness function that considers two crucial metrics. First, it aims to maximize the differences between the driving paths of the ego vehicle in the two scenarios, directly accentuating the non-optimal behaviors. Second, it quantifies the similarity of

the ego’s behavior, measured by a vector encompassing velocity, acceleration, and orientation. This metric is essential as the behavior of the ego vehicle directly influences the path it takes.

We have evaluated *Decictor* on the Baidu Apollo with its built-in SimControl [3]. Since there is no existing work focusing on optimal decision testing, we compared *Decictor* with two random methods, i.e., Random, which generates scenarios randomly, and Random- δ , which applies our non-invasive mutation and random selection to generate scenarios, and three state-of-the-art safety testing methods, i.e., AVFuzzer [23], SAMOTA [16], and BehAVExplor [6] on four meticulously validated ODSs. The evaluation results reveal the effectiveness and efficiency of *Decictor* in detecting NoDSs. Moreover, the comparison results emphasize the necessity of *Decictor* for optimal decision testing. Further experimental results demonstrate the utility of the mutation operation and feedback mechanisms meticulously designed within *Decictor*.

In summary, this paper makes the following contributions:

- (1) We are the first to investigate the problem of non-optimal decisions made by ADSs. Specifically, we propose a metamorphic relation that effectively exposes non-safety-critical issues related to decision-making in ADSs.
- (2) We develop a search-based algorithm that efficiently generates NoDSs, offering insights into non-safety-critical violations in ADSs.
- (3) We conduct extensive experiments to evaluate the effectiveness and usefulness of *Decictor* on Baidu Apollo. As a result, a total of 46.0 NoDSs is discovered based on four initial ODSs on average, demonstrating the potential and value of *Decictor* in detecting non-optimal decisions made by ADSs.

2 BACKGROUND AND NOTATION

2.1 Autonomous Driving Systems

ADSs control the behavior of autonomous vehicles, i.e., the ego vehicles. Existing ADSs mainly contain two categories: End-to-End (E2E) systems [19, 41], and module-based ADSs [3, 21]. E2E systems use united deep learning models to generate control decisions from sensor data directly. Recently, the rapid development of Deep Learning and Large Models have led to high-performance E2E systems in close-loop datasets, such as UniADS [19] and OpenPilot [7]. However, these E2E systems still perform poorly on unseen testing data, such as easily colliding with obstacles. In contrast, module-based ADSs have better performance in various scenarios.

A typical module-based ADS, such as Baidu Apollo [3] and Autoware [21], usually consists of localization, perception, prediction, planning, and control modules to generate decisions from rich sensor data. The localization module provides the location of the ego vehicle by fusing multiple input data from GPS, IMU, and LiDAR sensors. The perception module takes camera images, LiDAR point clouds, and Radar signals as inputs to detect the surrounding environment (e.g., traffic lights) and objects (e.g. other vehicles and pedestrians) by mainly using deep neural networks. The prediction module is responsible for tracking and predicting the trajectories of all surrounding objects detected by the perception module. Given the results of perception and prediction modules, the planning module then generates a local collision-free trajectory for the ego vehicle. Finally, the control module converts the planned trajectory

to vehicle control commands (e.g., steering, throttle, and braking) and sends them to the chassis of the vehicle. In this paper, we choose to test module-based ADSs on a simulation platform, where the ADS connects to a simulator via a communication bridge, receives sensor data from the simulator, and sends the control commands to the vehicle in the simulator.

2.2 Scenario

ADS testing necessitates a collection of scenarios as inputs. Each scenario is characterized by a specific environment (e.g., road, weather, and illumination) and the scenery and objects (static obstacles, Non-Player Character (NPC) vehicles, and pedestrians). In essence, a complex scenario can be generated by combining relevant attributes from the Operational Design Domains (ODDs) [35]. However, it is impractical to encompass all attributes with all possible values due to the vastness of the attribute space. Consequently, existing studies select different subsets of attributes for specific testing purposes. In this paper, we focus on evaluating the non-safety-critical performance of the motion generated by the ADS under test. As a result, we primarily employ traffic cones as static obstacles and NPC vehicles as dynamic objects to formulate our scenarios.

Scenario. A *scenario* can be described as a tuple $s = \{\mathcal{A}, \mathcal{P}\}$, where \mathcal{A} is the motion task of the ADS under test, including the start position and the destination, \mathcal{P} is a finite set of participants, including the set of static obstacles and dynamic NPC vehicles. Scenario observation is a sequence of scenes, and each scene represents the states of the ego vehicle and other participants at a timestamp. Formally, given a scenario $s = \{\mathcal{A}, \mathcal{P}\}$, its observation is denoted as $O(s) = \{s_0, s_1, \dots, s_k\}$, where k is the length of the observation and s_i is a scene at timestamp i . In detail, $s_i = \{y_i^0, y_i^1, \dots, y_i^{|\mathcal{P}|}\}$ where $y_i^j = \{p_i^j, \theta_i^j, v_i^j, a_i^j\}$ denotes the waypoint of a participant $j \in \mathcal{P}$ at timestamp i , including the center position p_i^j , the heading θ_i^j , the velocity v_i^j and the acceleration a_i^j . A driving path of the participant j can be defined as $\tau^j(s) = \{p_0^j, \dots, p_k^j\}$. By default, we use $\tau(s)$ to represent the driving path of the ego vehicle in the scenario s . Unless otherwise specified, the driving path in the following context refers to the path of the ego vehicle in s , i.e., $\tau(s)$.

3 OVERVIEW

3.1 Problem Definition

This paper deviates from conventional evaluation of ADSs that typically focus on safety-related requirements. Instead, we aim to assess the optimization capability of the decision-making process in ADSs. Given a scenario s and its associated potential optimal path for the ego vehicle, denoted as $\tau^*(s)$, our optimal decision testing endeavors to determine the ADS's ability to consistently navigate along $\tau^*(s)$.

Unfortunately, it is hard to evaluate the ego vehicle's driving path $\tau(s)$ is an optimal one due to the lack of testing oracles; that is, we do not know s 's optimal path of $\tau^*(s)$. Despite the possibility of manually assessing the driving path in each scenario, it becomes overwhelming, especially considering the multitude of scenarios involved in optimal decision testing. To address this, we employ metamorphic testing to detect the basic decision strategies. The metamorphic relation (MR) is defined as follows:

Definition 1 (Metamorphic Relation). Given an ODS $s = \{\mathcal{A}, \mathcal{P}\}$, we formalize the metamorphic relation as:

$$\forall P \subseteq \mathbb{P}, \epsilon(\tau(s), \tau(\delta(s, P))) = True \quad (1)$$

where $\mathbb{P}(\supseteq \mathcal{P})$ is the set of all possible participants in a scenario, the function τ retrieves the path that the ego vehicle takes in a scenario, and δ is a mutation function that modifies the behaviors of participants in P . It is crucial to note that the mutation function δ is designed in such a manner that even in the new scenario (i.e., $s' = \delta(s, P)$), the ego vehicle can still take the driving path in the scenario s . The function ϵ is an equality function that assesses the equivalence of two paths.

The MR essentially posits that, within a specified new scenario (i.e., $s' = \delta(s, P)$), the ADS should exhibit the ability to select the original optimal path. NoDSs can be identified by detecting violations of the MR. Note that the decision optimality of an initial scenario \hat{s} can be manually confirmed while the mutated scenarios can be automatically checked by the MR.

Challenges. Implementing the MR presents several challenges, particularly concerning the functions δ and ϵ . Not all mutated scenarios, i.e., $\delta(s, P)$, are suitable for the MR. One challenge lies in ensuring the ego vehicle can still traverse the original optimal path in the mutated scenario. For instance, if obstacles are introduced into the original optimal path, the ego vehicle may select a different path for safety considerations. While this new path differs from the original (i.e., $\tau(s)$), it may still be optimal within the context of the new scenario. The second challenge involves determining the path equivalence of two scenarios. The behavior of the ego vehicle may differ slightly between a NoDS and its corresponding ODS, such as minor differences between two paths. Even if they are not strictly identical, both paths could be optimal. Therefore, defining the function ϵ presents another challenge. Furthermore, once the MR is implemented, efficiently generating NoDSs that violate the MR remains challenging. To address these issues, this paper focuses on the development of the MR and the test generation algorithm.

3.2 Approach Overview

Figure 2 provides a high-level depiction of our testing framework *Decitor*, designed to detect non-optimal decisions using the metamorphic relation. The basic idea underlying our method involves generating a scenario s' , where the ego vehicle opts for a path that is far from the optimal path in s . It can be formulated as an optimization problem aiming to maximize the difference between the driving paths or behaviors of s and s' :

$$\Delta_s = \arg \max_{\Delta} \mathcal{D}(\tau(s), \tau(s')), \text{ s.t., } s' = \delta(s, \Delta), \quad (2)$$

where Δ symbolizes the metamorphic relation-compliant perturbation on the scenario s , and \mathcal{D} represents a feedback function used to measure the distance or difference between the driving paths or behaviors of the two scenarios. Therefore, we can generate the NoDS from $s: s' = \delta(s, \Delta_s)$.

Decitor adopts a search-based method to solve the optimization problem. The process initiates with an initial ODS \hat{s} and aims to output a set of MR failure tests, i.e., NoDSs. We first initialize a population \mathcal{Q} based on \hat{s} . *Decitor* then optimizes this population

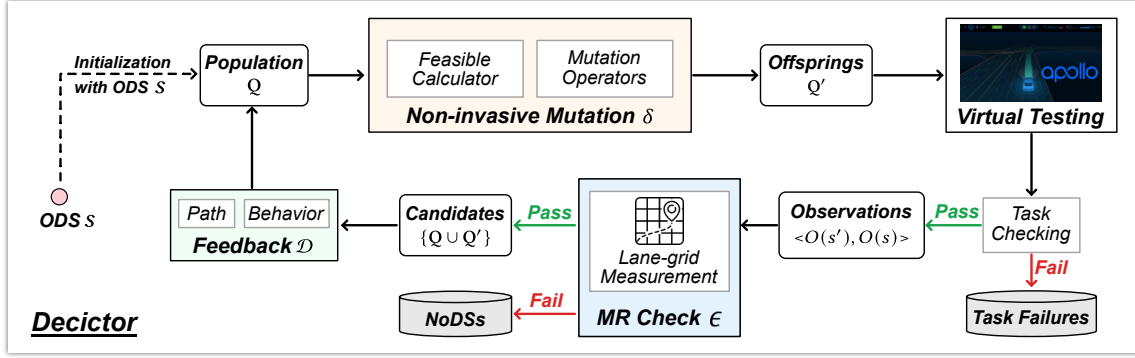


Figure 2: Overview of Decictor.

iteratively until the testing budget B exceeds. In each iteration, *Decictor* performs *Non-invasive Mutation* (δ) to generate the offspring Q' that has the same size as Q . To comply with the constraints of the MR, the mutation strategy ensures that the original optimal path in s remains available in the new scenarios. To determine if the ADS makes optimal driving decisions in these new scenarios, we introduce *MR Check* (ϵ), a hierarchical approach for measuring equivalence between the initial ODS and these new scenarios. *MR Check* initially monitors whether a new scenario has completed the task in virtual testing. If the new scenario fails this test, it is identified as a task failure and subsequently not regarded as a NoDS. Conversely, if the new scenario passes the task checking, we collect the observation including the driving path from the simulator. The *MR Check* then verifies the equivalence of the driving paths between the initial ODS and the new scenario by using a lane-grid measurement. Detection of the MR violation in this step identifies a NoDS. If no violation occurs, *Decictor* proceeds to select the superior population from the candidates of the old and new populations for the next iteration. This selection process is guided by a *Feedback* (\mathcal{D}) that takes into account the spatial and temporal characteristics, i.e., the driving path and the behaviors, of the ego vehicle's motion.

4 APPROACH

Algorithm 1 presents the main algorithmic procedure of *Decictor*. *Decictor* receives a seed ODS s as the input and outputs a set of NoDSs violated the metamorphic relation. Parameters N and B can be adjusted to configure the population size and testing budget, respectively. The algorithm begins by creating an initial population with the given initial ODS \hat{s} (Lines 2-3). In each iteration, the algorithm first generates the offspring by mutating each scenario in the population Q (Lines 6-7). Each new scenario s' is first executed by the virtual testing (Line 8) and verified by the task checking (Line 9). The new scenario passed the task checking is then evaluated for the satisfiability of the MR (Lines 10-14). If the MR is violated, a NoDS is identified and added to the set F_n (Line 14). If no MR violation is detected, the new scenario is added to the offspring Q' . The scenario selection process then commences, which involves picking the top N scenarios from the union of Q and Q' based on their fitness scores (Line 15). The algorithm ends by returning detected NoDSs F_n (Line 17).

Algorithm 1: Decictor Algorithm

```

Input      : An initial seed ODS  $\hat{s}$ 
Output    : A set of NoDSs  $F_n$ 
Parameters: Population size  $N$ , Testing budget  $B$ 
1  $F_n \leftarrow \{\}, Q \leftarrow \{\}$ 
2 for  $i \in \{1, \dots, N\}$  do
3    $Q \leftarrow Q \cup \{\hat{s}\}$ 
4 repeat
5    $Q' \leftarrow \{\}$ 
6   for  $s \in Q$  do
7      $s' \leftarrow \delta(s, \Delta)$  // Non-invasive Mutation
8      $r_{ot}, O(s') \leftarrow \text{VirtualTest}(s')$ 
9     if  $r_{ot}$  is pass then
10      // MR Check
11       $r_{mr} \leftarrow \epsilon(\tau(s), \tau(s'))$ 
12      if  $r_{mr}$  is pass then
13         $Q' \leftarrow Q' \cup \{s'\}$ 
14      else
15         $F_n \leftarrow F_n \cup \{s'\}$ 
16    $Q \leftarrow \text{Selection}(\{Q \cup Q'\}, N)$  // Feedback
17 until Testing budget  $B$  exhausted;
18 return  $F_n$ 

```

In the following sections, we introduce the key components of *Decictor*: the *Non-invasive Mutation* (δ), the *Metamorphic Relation Check* (ϵ), and the *Feedback* (\mathcal{D}).

4.1 Non-invasive Mutation δ

The main challenge of the mutation is to ensure that in the mutated scenario, the optimal path of the ego vehicle from the seed ODS is not affected. However, existing mutation techniques for ADS safety testing typically alter the waypoints of NPC vehicles [6, 16, 23, 34], which could significantly impact the ego vehicle's optimal path in the original ODS. To address these limitations, we propose a non-invasive mutation that effectively generates mutated scenarios without disrupting the optimal path of the ODS. The non-invasive mutation mainly includes *adding* new participants within the non-invasive feasible areas and *removing* existing added participants.

Non-invasive Feasible Area. To guarantee non-invasion, we aim to compute a set of *non-invasive feasible areas* such that the

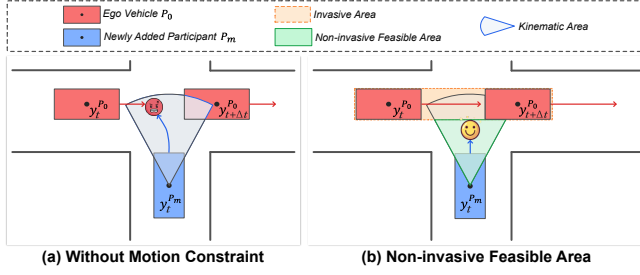


Figure 3: Illustrative example of feasible area calculation.

newly added participant P_m will not affect the motion of the ego vehicle and other participants if P_m moves around in these non-invasive feasible areas. Note that it is essential that the motions of other participants remain unaffected, as their behaviors could indirectly alter the motion of the ego vehicle.

Given an ODS $s = \{\mathcal{A}, \mathcal{P}\}$ and the observation $O(s) = \{s_0, s_1, \dots, s_k\}$ with a sampling time step Δt , we define the non-invasive feasible area regarding to $p \in \{\mathcal{P} \cup P_0\}$ for the next timestamp $t + \Delta t$ as $R_p(s, t, \Delta t)$, where P_0 is the ego vehicle.

Figure 3 illustrates the basic idea about the computation of $R_p(s, t, \Delta t)$, taking the ego vehicle as an example. First, the new participant should move in the feasible motion area, denoted as $R(y_t)$, according to its kinematic constraints (e.g., the maximal speed and steering angle) and the position y_t at timestamp t , i.e., the sector in Figure 3(a). Second, suppose the motion area of the ego vehicle P_0 between $[t, t + \Delta t]$ is $R^{P_0}(s_t, s_{t+\Delta t})$, e.g., the dashed light orange area in Figure 3(b). $R^{P_0}(s_t, s_{t+\Delta t})$ can be determined as P_0 's motion area from s_t to $s_{t+\Delta t}$ in the ODS s . Clearly, the new participant should not move into $R^{P_0}(s_t, s_{t+\Delta t})$ during $[t, t + \Delta t]$. Therefore, we have

$$R_{P_0}(s, t, \Delta t) = R(y_t) \setminus R^{P_0}(s_t, s_{t+\Delta t}), \quad (3)$$

i.e., the light green area in Figure 3(b).

Consequently, the non-invasive feasible area for the newly added participant at timestamp $t + \Delta t$ is:

$$R(s, t, \Delta t) = \bigcap_{p \in \{\mathcal{P} \cup P_0\}} R_p(s, t, \Delta t) \quad (4)$$

where $R_p(s, t, \Delta t)$ is the non-invasive feasible area regarding to participant p , and P_0 is the ego vehicle.

It is worth noting that the time step Δt will affect the computation of the non-invasive area and the detection of NoDSs significantly. As Δt increases, the non-invasive area becomes more conservative, leading to fewer detected NoDSs.

Mutation Operations. Algorithm 2 outlines the specific mutation operations: *Adding* (Lines 1-11) and *Removing* (Lines 12-15). The non-invasive mutation takes as input $\mathcal{P}_{\hat{s}}$ (the participants in the initial ODS \hat{s}), \mathcal{P}_s (the participants in the current ODS s) and $O(s)$ (the observation of s). The observation consists of a sequence of scenes $\{s_0, \dots, s_k\}$ with an equal time step Δt . In each iteration, the non-invasive mutation randomly chooses one operation to change participants in the scenario s , resulting in a new scenario s' .

Adding. Adding operation aims to introduce complexity to the scenario by adding a new participant to s without influencing the optimal path. In detail, this operation initializes an empty waypoint set P_m and a collision-free waypoint y_0 (Lines 2-3). Waypoints for

Algorithm 2: Non-invasive Mutation Operators

Input : Participants in the initial ODS \hat{s} : $\mathcal{P}_{\hat{s}}$
Participants in the current ODS s : \mathcal{P}_s
Observation of s : $O(s) = \{s_0, s_1, \dots, s_k\}$

Output : Participants in the newly mutated scenario s' : $\mathcal{P}_{s'}$

Parameters: Time step Δt between two successive waypoints.

- 1 **Function Adding()**:
- 2 $P_m \leftarrow \{\}$
- 3 $y_0 \leftarrow$ a collision-free waypoint with zero speed
- 4 **for** $t \in \{0, 1, 2, \dots, k-1\}$ **do**
- 5 $R(s, t, \Delta t) \leftarrow$ **NonInvasiveArea**($y_t, O(s), \Delta t$)
- 6 **if** $R(s, t, \Delta t)$ is \emptyset **then**
- 7 **return** \emptyset
- 8 $y_{t+\Delta t} \leftarrow$ **Sample**($R(s, t, \Delta t)$)
- 9 $P_m \leftarrow P_m \cup \{y_{t+\Delta t}\}$
- 10 $\mathcal{P}_{s'} \leftarrow \mathcal{P}_s \cup \{P_m\}$
- 11 **return** $\mathcal{P}_{s'}$
- 12 **Function Removing()**:
- 13 $P_m \leftarrow$ **Sample**($\mathcal{P}_s \setminus \mathcal{P}_{\hat{s}}$)
- 14 $\mathcal{P}_{s'} \leftarrow \{\mathcal{P}_s \setminus P_m\}$
- 15 **return** $\mathcal{P}_{s'}$

the added participant are iteratively generated (Lines 4-9), where each iteration involves calculating the non-invasive area (Line 5), sampling a non-invasive waypoint (Line 6-8), and adding it to P_m (Line 9). The process concludes by merging the resultant set with the original participants \mathcal{P}_s to form $\mathcal{P}_{s'}$ (Line 10-11).

Removing. Continuously adding new participants to the scenario will introduce too many obstacles, resulting in motion task failures. Therefore, we introduce the removing operator in this paper. Note that only the participants in $\mathcal{P}_s \setminus \mathcal{P}_{\hat{s}}$, i.e., the participants newly added to the initial ODS, can be removed, while the participants in the initial ODS will remain unchanged in all mutated scenarios. The reason is that the removal of the participants in the initial ODS may affect the optimal path of the scenarios. Specifically, this operation removes a participant in $\mathcal{P}_s \setminus \mathcal{P}_{\hat{s}}$ randomly (Lines 13-14) and returns the mutated set (Line 15).

4.2 MR Check ϵ

Given an ODS s and a mutated scenario s' , we require a criterion ϵ to determine whether s' remains an ODS. A direct approach might be checking if the driving path in s' (i.e., $\tau(s')$) and the original path of s (i.e., $\tau(s)$) are the same. However, it can be overly strict, as $\tau(s')$ can still be considered optimal even if it slightly deviates from the original path $\tau(s)$ (e.g., the path in Figure 4(b) can still be regarded as an optimal one). To address this, we propose an abstraction-based method to quantify the similarity between the two driving paths.

Figure 4 illustrates the basic idea of our method. We define an optimal area around the optimal path $\tau(s)$ in terms of the grid map. Any driving path falling or mostly falling within this area is considered optimal and satisfies the MR. For example, the green area in Figure 4(a) defines the optimal area of the driving path in the ODS. The driving path in Figure 4(b) lies in the optimal area, resulting in the highest similarity, and thus meets the MR

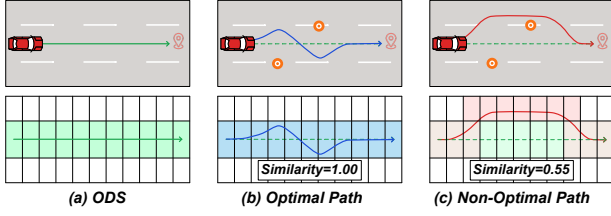


Figure 4: MR checking with grid map. The above are the driving paths and the below are the locations of the corresponding paths in the grid map.

criterion, while most of the path in Figure 4(c) (i.e., the red area) falls outside the optimal area, resulting in a low similarity, and the MR is violated.

Specifically, the comparison between the driving path $\tau(s)$ and the driving path $\tau(s')$ is implemented by a grid-based approach, as shown in Figure 4. The map is divided into grids, and each driving path is mapped to a set of grids. Technically, a driving path of the ego vehicle is represented as a sequence of locations $\tau(s) = \{p_0^0, \dots, p_k^0\}$, where p_i^0 is the position at frame i . To collect the covered grids, a function g is used to map each position p to the grid where it is located. The covered grids for the path $\tau(s)$ can be denoted as:

$$C_{\tau(s)} = \{g(p) \mid p \in \tau(s)\} \quad (5)$$

To check the MR, the similarity between the covered grids of $\tau(s)$ and $\tau(s')$ is computed. The MR checking is defined using a predefined threshold ϵ as follows:

$$\epsilon(\tau(s), \tau(s')) = \frac{|C_{\tau(s)} \cap C_{\tau(s')}|}{|C_{\tau(s)} \cup C_{\tau(s')}|} > \epsilon \quad (6)$$

If the similarity between the covered grids is greater than the threshold ϵ , the MR is satisfied and s' is recognized as an ODS.

4.3 Feedback \mathcal{D}

To guide the search of NoDSs, a feedback is necessary to select high-quality individuals from the candidate population (Line 15 of Algorithm 1). The grid similarity $\epsilon(\tau(s), \tau(s'))$ (in Equation 6) provides a direct choice for the feedback. However, the calculation of grid similarity is relatively coarse-grained as it only considers the spatial perspective of the ego vehicle's motion. While this coarse-grained calculation is beneficial for MR checking, as it considers different possible optimal paths, it may not be as specific and effective for guiding the testing process to generate NoDSs (see the evaluation results in Section 5.2.2). To address this, another fitness is proposed that incorporates more fine-grained feedback from both the driving path and the behavior of the ego vehicle. The former focuses on the spatial characteristics of the ego vehicle's motion, while the latter more on the temporal ones.

Driving Path Feedback. The main objective of *Decictor* is to maximize the difference between the driving paths such that MR is not satisfied. Considering the potential different lengths of $\tau(s)$ and $\tau(s')$, we use the shortest distance between $\tau(s)$ and $\tau(s')$ in the spatial space to measure their difference. A larger distance indicates a higher likelihood that the MR will be violated. The distance is

calculated based on the point-wise distance:

$$f_p(s, s') = \frac{1}{n_{s'}} \sum_{i=1}^{n_{s'}} \min(\{\|p_i - p\| \mid \forall p \in \tau(s)\}) \quad (7)$$

where $p_i \in \tau(s')$ and $n_{s'}$ is the total number of points in $\tau(s')$.

Behavior Feedback. In some cases, optimizing only the driving path feedback might be insufficient (see the experimental results in Section 5.2.2), so an additional feedback mechanism is provided, which relies on the behavior of the ego vehicle. This behavior feedback considers factors such as the ego's velocity, acceleration, and heading. By analyzing the ego's behavior, it becomes possible to gain insights into how slight changes in behavior could lead to variations in the driving path and increase the overall difference between $\tau(s)$ and $\tau(s')$. For example, if the heading of the ego vehicle changes slightly, it may not directly cause a significant increase in driving path differences. However, such a change could serve as a valuable indicator, as altering the heading or acceleration of the ego vehicle could lead to adjustments in the driving path, potentially resulting in an increased difference between paths.

To implement this behavior feedback, the ego's behavior is collected from its waypoints in the scenario s , denoted as

$$X_s = ((v_0, a_0, \theta_0), (v_1, a_1, \theta_1), \dots, (v_k, a_k, \theta_k))$$

where v_i , a_i , and θ_i represent the velocity, acceleration, and heading at timestamp i , respectively. To compare the behavior differences between two scenarios s and s' , the Maximum Mean Discrepancy (MMD) is used as the measure of distance between their behavior distributions. The MMD is a widely used statistical metric for comparing distributions and can effectively quantify differences between two sets of data. The behavior feedback function $f_b(s, s')$ is defined as follows:

$$f_b(s, s') = f_{MMD}(X_s, X_{s'}). \quad (8)$$

Finally, the fitness of s' in relation to the ODS s is calculated as:

$$\mathcal{D}(\tau(s), \tau(s')) = f_p(s, s') + f_b(s, s'). \quad (9)$$

5 EMPIRICAL EVALUATION

In this section, we aim to empirically evaluate the capability of *Decictor* on NoDS generation. In particular, we will answer the following research questions:

RQ1: Can *Decictor* effectively find NoDSs for ADSs in comparison to the baselines?

RQ2: How useful are the Non-invasive Mutation and the feedback designed in *Decictor*?

RQ3: How does *Decictor* perform from the perspective of time efficiency?

To answer these research questions, we conduct experiments using the following settings:

Environment. We implement *Decictor* with Baidu Apollo 7.0 [3] and its built-in simulation environment SimControl. Baidu Apollo 7.0 is an open-source and industrial-level ADS that supports a wide variety of driving supports.

Driving Scenarios. We evaluate *Decictor* on a real-world Map Sunnyvale Loop, provided as part of Baidu Apollo. Similar to [6, 23], we manually choose four basic representative scenarios and build the initial ODSs, the inputs of Algorithm 1. These basic scenarios

Table 1: Comparison results with baselines.

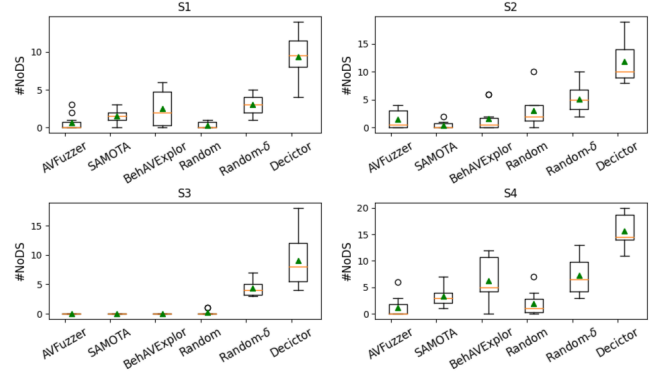
Method	%Mutation \uparrow					#NoDS (#NoDS-Hum) \uparrow				
	S1	S2	S3	S4	Avg.	S1	S2	S3	S4	Sum
AVFuzzer	41.5	40.5	70.6	10.6	40.8	0.6 (0.3)	1.5 (1.0)	0.0 (0.0)	1.2 (0.5)	3.3 (1.8)
SAMOTA	58.6	50.1	49.6	55.7	53.4	1.5 (0.9)	0.4 (0.3)	0.0 (0.0)	3.3 (1.2)	5.2 (2.4)
BehAVExplor	29.7	36.3	36.6	32.1	33.6	2.5 (1.7)	1.6 (0.7)	0.0 (0.0)	6.3 (2.3)	10.4 (4.7)
Random	73.2	73.1	70.2	76.7	73.3	0.3 (0.0)	3.0 (1.5)	0.2 (0.2)	1.9 (0.7)	5.4 (2.4)
Random-δ	96.4	97.4	99.0	96.0	97.2	3.0 (1.4)	5.1 (4.6)	4.4 (4.4)	7.2 (2.0)	19.7 (12.4)
Decictor	98.0	97.5	99.4	97.5	98.1	9.4 (3.9)	11.9 (8.6)	9.0 (9.0)	15.7 (6.7)	46.0 (28.2)

have been widely tested in previous literature [6, 16, 23, 35, 43]. As shown in the left column of Figure 6, the selected ODSs include left turn (S1), right turn (S2), lane following (S3) and U-turn (S4). All initial ODSs are manually confirmed.

Baselines. In this paper, we selected five baseline methods including Random, Random- δ , AVFuzzer [23], SAMOTA [16], and BehAVExplor [6]. Specifically, we implemented two Random strategies: 1) Random, which does not have any feedback and mutation constraints. It randomly generates scenarios by adding or removing dynamic vehicles or static obstacles; 2) Random- δ , which does not have feedback but uses our non-invasive mutation δ . To the best of our knowledge, this is the first paper to specifically evaluate the optimality of decision-making, and there are no direct baselines. Consequently, we understand that comparisons with the three other baselines, primarily designed for identifying safety-critical violations, may not be entirely fair. However, while not their primary focus, they can still generate scenarios with suboptimal decisions. Comparison with these tools can still underscore the need for specialized tools such as *Decictor* to test the optimality of decisions. Note that these three baselines are originally evaluated on the simulator LGSVL [31]. Due to the official sunset of LGSVL [22], we customize them to our simulation environment (i.e., SimControl + Apollo) for comparison.

Metrics. To facilitate comparison with the baseline techniques, we have incorporated our MR into them to gather the generated NoDSs. In our experiments, we utilize the metrics #NoDS and #NoDS-Hum to assess the effectiveness of NoDS generation. #NoDS quantifies the number of potential NoDSs, identified through our MR checking with a predetermined threshold ϵ . To address the inherent subjectivity in determining (non-)optimal decisions, we introduce #NoDS-Hum, which represents the number of NoDSs validated by human assessment. Here, the co-authors independently verify whether each NoDS is truly a non-optimal decision. A NoDS is only counted in #NoDS-Hum if all authors unanimously recognize it as non-optimal, indicating a clear-cut case of a non-optimal decision. It's important to note that scenarios excluded from #NoDS-Hum don't necessarily indicate they are still optimal decisions; rather, it means at least one participant was uncertain about the non-optimality. The scenarios not adhering to the non-invasive mutation will be filtered directly, owing to the absence of verifiable ground truth. Moreover, we also assess the success rate of non-invasive mutations, denoted as %Mutation. The evaluation involves replaying the path of the ego vehicle in each mutated scenario alongside the optimal path of the ODS and verifying the completion of the motion task.

Implementation. Following AVFuzzer [23], we set the population size N in *Decictor* to 4. In our mutation, we consider both dynamic

**Figure 5: Comparison of #NoDS for different tools.**

vehicles and static obstacles (i.e., traffic cones). The time step Δt in the non-invasive mutation is set to 2s. In MR check, the equality threshold ϵ is empirically set to 0.6, and the grid size is set to 2 meters. Similar to previous works [16, 17], we repeat each experiment 10 times and report statistics over these runs. For each run, we used the same budget of four hours, as we found that it was long enough to compare based on our preliminary evaluation.

5.1 RQ1: Effectiveness of *Decictor*

5.1.1 Comparative Results. Table 1 compares %Mutation, #NoDS, and #NoDS-Hum across four initial ODSs: S1, S2, S3, and S4, and Figure 5 shows the distribution of #NoDS, where the median and the average are represented by an orange bar and a green triangle, respectively. From the results, we can find that *Decictor* outperforms the baselines in #NoDS and #NoDS-Hum. In detail, on average of #NoDS, *Decictor* outperforms the best baseline (i.e., Random- δ): S1 (9.4 vs. 3.0), S2 (11.9 vs. 5.1), S3 (9.0 vs. 4.4), and S4 (15.7 vs. 7.2). Among all the detected NoDSs by *Decictor*, we finally identified 3.9, 8.6, 9.0, and 6.7 NoDS-Hum in S1, S2, S3, and S4, respectively. Even with very rigorous manual filtering, *Decictor* still significantly outperforms the best baseline (Random- δ). The results indicate the effectiveness of *Decictor* in identifying NoDSs and NoDS-Hum. We further observed that Random- δ outperforms both the Random (19.7 vs. 5.4 for the total number of NoDSs) and other three safety-oriented baselines (19.7 vs. 3.3, 5.2, and 10.4 in Sum of #NoDS). This is attributed to the effectiveness of the non-invasive mutation used in Random- δ and *Decictor*. Regarding %Mutation (Avg. column), Table 1 reveals that Random and safety-oriented baselines produce a maximum of 73.3% valid mutations (i.e., the original optimal path

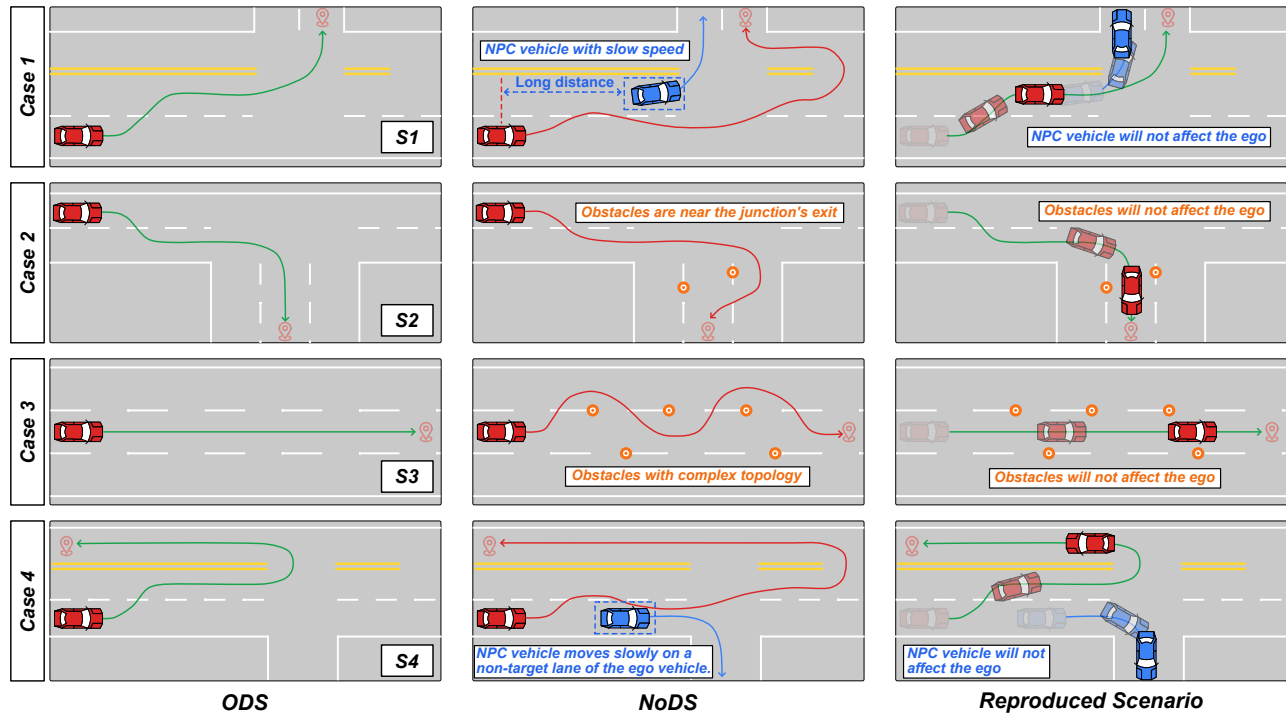


Figure 6: Samples of NoDSs detected by Decictor. The red vehicle is the AV. Optimal paths are indicated in green, while non-optimal paths are displayed in red. The first column is the initial ODSs, the second column shows the corresponding NoDSs, and the last column depicts the reproduced scenarios validating that the original optimal paths can be traversed in the NoDSs.

is not affected), which is significantly lower than non-invasive mutation methods (97.2% for Random- δ and 98.1% for *Decictor* on average). Therefore, they are not effective in detecting NoDSs. The comparison of results between Random- δ and *Decictor* highlights the effectiveness of the feedback mechanism in *Decictor*. BehAV-Explor performs better than the other two safety-guided baselines due to its diversity feedback mechanism, enabling it to generate scenarios with a wide range of behaviors. As a result, it has a higher likelihood of generating NoDSs.

In summary, the comparison of *Decictor* with Random and Random- δ demonstrates its effectiveness in detecting NoDSs. When contrasted with the three safety-oriented baselines, the results emphasize the importance of robust decision-making testing. In fact, *Decictor* and existing safety-oriented baselines are complementary, given their distinct testing objectives.

5.1.2 Case Study. Figure 6 showcases four NoDS examples generated from the four initial ODSs. Each example includes three scenarios: the initial ODS, the identified NoDS, and the reproduced scenario (i.e., the optimal decision in the NoDS). The examples illustrate that the ego vehicle takes non-optimal paths in the detected NoDSs, even though the optimal ones are still available. Details are explained as follows:

Case 1. Inaccurate Prediction on Vehicle Status. *Decictor* adds a new NPC vehicle with a low initial speed in the NoDS. Despite being initially placed on the ego vehicle’s optimal path and far away, the NPC vehicle will have moved by the time the ego

vehicle reaches that segment. The original optimal path remains available, as shown in the reproduced scenario. However, the ADS makes an incorrect prediction, considering the NPC vehicle as stationary. Consequently, it stops lane changing and chooses a less efficient path.

Case 2. Inaccurate Prediction on Obstacle Impact. *Decictor* introduces two obstacles along the lane boundaries near the exit of the junction. These two obstacles do not influence the optimal path. In this NoDS, the ego vehicle incorrectly assesses that the target lane is impassable. Consequently, it chooses to approach the destination from an adjacent, external lane. This choice is not optimal and introduces significant risks within the context of real-world traffic.

Case 3. Inaccurate Prediction on Safe Regions. *Decictor* introduces five static obstacles in the NoDS, without disrupting the optimal path (as shown in the reproduced scenario). However, the ego vehicle deviates from the optimal path and chooses an alternative path to reach the destination. It involves navigating around the obstacles and changing lanes four times, leading to a non-smooth and dangerous motion. This scenario illustrates the ADS’s insufficient intelligence, resulting in non-optimal decisions.

Case 4. Inaccurate Prediction on Vehicle Intention. *Decictor* introduces a new NPC vehicle in the NoDS. Note that this NPC vehicle does not intersect with the optimal path of the ego vehicle. The NPC vehicle travels along the blue path at a low speed. However, the ego vehicle incorrectly predicts that the NPC vehicle intends to change to the left lane. This misinterpretation causes the ego

Table 2: Comparison of mutations.

Method	%Mutation \uparrow					#NoDS \uparrow				
	S1	S2	S3	S4	Avg.	S1	S2	S3	S4	Sum
w/o Cons	71.7	71.3	74.8	65.5	70.8	2.7	4.5	1.6	5.7	14.5
w/o Mot	71.1	80.9	98.6	68.9	79.9	4.0	8.6	5.2	10.8	28.6
w/o Rem	97.5	97.3	99.4	97.2	97.9	3.9	9.3	4.9	9.1	27.2
Decictor	98.0	97.5	99.4	97.5	98.1	9.4	11.9	9.0	15.7	46.0

vehicle to focus excessively on the NPC’s movement, leading it to overlook the inadequate available space to execute a left turn. As a result, the ego vehicle is compelled to select a non-optimal path to reach its destination.

Answer to RQ1: *Decictor* significantly outperforms existing methods in identifying NoDSs. While conventional ADS testing methods primarily focus on detecting safety issues, *Decictor* can serve as a complement to them for a more comprehensive evaluation of ADSs.

5.2 RQ2: Usefulness of Mutation and Feedback

We assess the usefulness of the key components in *Decictor*, i.e., the *non-invasive mutation* and the *feedback* mechanism. To achieve this, we conducted a thorough evaluation by configuring a series of variants of *Decictor* and then proceeded to evaluate their usefulness.

5.2.1 Mutation. For mutation, we compared *Decictor* with its three variants: (1) *w/o Cons* applies a random mutation instead of the non-invasive mutation in *Decictor*, aiming to evaluate the effectiveness of the non-invasive mutation; (2) *w/o Mot* sets the time step to 0s in the calculation of non-invasive feasible areas (i.e., only considering the motion constraint at each timestamp), aiming to measure the influence of the motion constraint between two successive timestamps. (3) *w/o Rem* uses only the adding operation in *Decictor* under the constraint of non-invasive mutation, aiming to assess the effectiveness of the combination of the two mutation operations, i.e., adding and removing participants. As shown in Table 2, we find that *w/o Cons* generates the fewest valid mutations (70.8%) and detects the smallest number of NoDSs (14.5), underlying the importance of the non-invasive mutation. Comparing *w/o Mot* with *Decictor*, we observed that only considering the motion constraint at each timestamp is insufficient, and the continuous-time motion constraint plays a significant role in calculating the non-invasive feasible area. Our preliminary experiments revealed that %Mutation increases while the #NoDS decreases as the time step increases. The reason is that a long time step will yield scenarios with reduced interactivity between the ego vehicle and the added participant, thus exerting a lower impact on the decision-making process of the ADS. Comparing *w/o Rem* and *Decictor*, we found that mutation with only the adding operation is more likely to induce more invalid mutations and a lower number of NoDSs. This is because the adding operation brings too many obstacles and may cause the failure of the motion task. Thus, the removing operation is also important for generating NoDSs.

Table 3: Comparison of feedback.

Method	#NoDS				
	S1	S2	S3	S4	Sum
F-Random	3.0	5.1	4.4	7.2	19.7
F-MR	3.0	6.7	1.2	7.5	18.4
F-Path	4.3	10.8	5.0	10.6	30.7
F-Behavior	5.3	9.0	5.4	11.5	31.2
Decictor	9.4	11.9	9.0	15.7	46.0

5.2.2 Feedback. For feedback, we implemented four variants: 1) *F-Random* replaces the feedback of *Decictor* with a random selection (from $Q \cup Q'$) to evaluate the effectiveness of our feedback strategy. 2) *F-MR* replaces the feedback of *Decictor* with the grid similarity used in our MR checking (see Equation 6) to compare the performance between using a coarse-grained grid distance and a fine-grained path distance. 3) *F-Path* and *F-Behavior* consider only the *driving path feedback* and the *behavior feedback*, respectively, to evaluate the usefulness of either feedback type.

Table 3 shows the experimental results of #NoDSs. The comparative results between *F-Random* and *Decictor* (19.7 vs. 46.0 in total) illustrate the effectiveness of the feedback used in *Decictor*. The results of *F-MR* (18.4) indicates that the grid similarity is not an effective feedback metric, as it may overlook some scenarios with a high probability of inducing NoDSs. From the ablation results of *F-Path* and *F-Behavior* (30.7 and 31.2, respectively), we see that both *behavior feedback* and *driving path feedback* are beneficial for detecting NoDSs. Their combination achieves the best performance.

Answer to RQ2: Both the non-invasive mutation and the two types of feedback are useful for *Decictor* to detect non-optimal decisions.

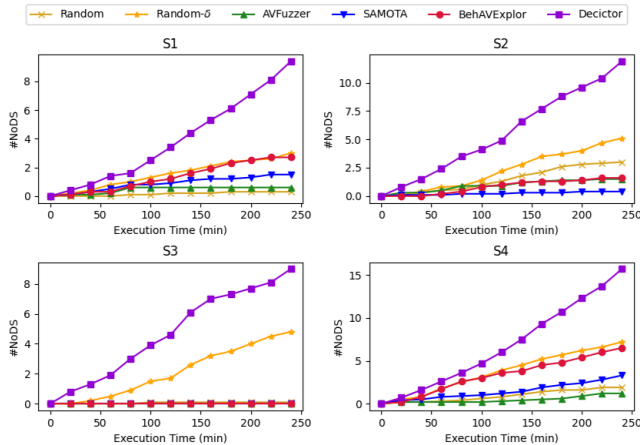
5.3 RQ3: Test Efficiency of *Decictor*

Figure 7 shows the cumulative number of NoDSs over the execution time of different methods. We can find that as *Decictor* continues its execution, the detection of NoDSs steadily increases, whereas other methods quickly reach a stable state. We further assess the time performance of different components in *Decictor*, including the overhead of mutation, oracle checking, feedback calculation, and simulation. Specifically, we analyze the average time to handle a scenario. The results are summarized in Table 4, where the columns *Mutation*, *Oracle Check*, *Feedback*, and *Simulation* represent the average time taken by a scenario for mutation, validity checking, fitness computation, and running the scenario in the simulation platform, respectively. 0.01* represents that the time cost is small, i.e., less than 0.01. For Random, the oracle and feedback stages are not involved, being marked as ‘N/A’.

The overall results show that, for all tools, the simulation process spends the majority of time. For instance, on average, *Decictor* takes 77.58 seconds to process a scenario, where 67.20 seconds (86.62%) are used in running the scenario. *Decictor* spends slightly more time in Mutation and Oracle Check than others due to the computation of the non-invasive feasible area for each waypoint and the grid-based similarity-checking mechanism. However, the computation time of *Decictor* remains within an acceptable range. SAMOTA consumes the most time in the feedback due to the necessity of training a

Table 4: Results of time performance (s)

Method	Mutation	Oracle Check	Feedback	Simulation	Total
Random	2.28	N/A	N/A	66.67	68.95
Random- δ	8.04	N/A	N/A	65.30	73.34
AVFuzzer	1.46	0.01*	0.01*	71.26	72.74
SAMOTA	1.18	0.01*	32.11	65.05	98.35
BehAVExplor	0.56	0.01*	1.41	77.06	79.04
Decictor	8.03	1.62	0.73	67.20	77.58

**Figure 7: #NoDSs over the execution of different methods.**

surrogate model. The differing time durations for simulation across various tools can be attributed to the different scenarios each tool generates (e.g., time-out scenarios), which in turn require varying amounts of simulation time.

Answer to RQ3: *Decictor* demonstrates efficiency, with the majority of the time (86.62%) spent in the simulation phase, while the main algorithmic component consumes approximately 10.38 seconds (13.38%).

5.4 Threats to Validity

Decictor suffers from some threats. The selection of the initial ODSs could potentially influence the results. To mitigate this, we have judiciously selected four motion tasks and created corresponding scenarios. Each scenario was run multiple times, with the optimal motion validated through both numerical analysis and expert judgment. Despite the MR Check ϵ in *Decictor*, the manual confirmation of NoDS-Hum may present another threat as different people may identify a scenario as either an ODS or a NoDS. To counter this, on one hand, we carefully select the threshold ϵ in the MR Check and Δt in the computation of non-invasive feasible area to reduce the number of such scenarios; on the other hand, to ensure robustness and consistency, all co-authors independently review the generated NoDSs, and only those confirmed by unanimous agreement among all authors will be considered in NoDS-Hum. Randomness may also be a threat to our results, and we mitigate the threat by repeating the experiment multiple times. Another potential threat could be that our current MR primarily addresses non-optimal decisions related to selecting inefficient paths. However, there can be other

types of non-optimal decisions, such as lack of smooth driving or unnecessary jittery movements, which are not considered by our current MR. In the future, we plan to extend the MR (e.g., considering velocity and acceleration) to detect more non-optimal decisions. Lastly, the customization of baselines to the Apollo+SimControl simulation environment could potentially affect the results. However, we only modified the interface between the algorithms and the simulation environment, leaving the algorithms themselves untouched. Moreover, to ensure the correctness, all co-authors thoroughly reviewed the code.

6 RELATED WORK

Safety-Guided ADS Testing. Safety plays the most important role in the development of ADSs. However, guaranteeing everlasting safety is challenging and many approaches have been proposed to generate safety-critical scenarios for evaluating the safety of ADSs. They can be divided into data-driven approaches [8, 11, 26–28, 30, 40] and searching-based approaches [6, 12, 15, 16, 18, 23, 32–34, 42, 43]. Data-driving methods produce critical scenarios from real-world data, such as traffic recordings [8, 28, 30] and accident reports [11, 26, 27, 40]. Search-based methods use various technologies to search for safety-critical scenarios from the scenario space, such as guided fuzzing [6, 23, 29], evolutionary algorithms [12, 15, 32–34, 43], surrogate models [16, 42], reinforcement learning [10, 17] and reachability analysis [2, 18]. All these methods aim to generate critical scenarios for evaluating ADSs’ safety-critical requirements, such as collision avoidance and reaching the destination. In contrast, our work focuses on evaluating the non-safety-critical requirements of ADSs, which is also crucial for the real-world deployment of ADSs. To the best of our knowledge, it is the first one considering the non-safety-critical requirements of ADSs.

Metamorphic Testing for ADS. Metamorphic testing (MT) has been an emerging approach to generating test cases and overcoming the oracle problem [5, 38]. Recently, MT has also been applied to test deep learning systems, such as the perception system of ADSs [37] and end-to-end deep learning-based ADSs [9, 36, 39]. For example, the authors in [36] designed an MR to test the robustness of an object detection system, which can be roughly described as: Inserting an additional object that does not overlap with preexisting objects in the source image should not affect the detection of the preexisting objects in the new image. However, there is only a little work focusing on MT for multi-module ADSs [14, 44]. In [14], the authors propose an MT method to identify avoidable collision scenarios, which means there are genuine failures in the ADS under test. In contrast to existing MT techniques that primarily focus on the correctness and safety of the system under test, we propose an MT method to detect vital non-safety-critical violations of the ADS under test.

7 CONCLUSION

In this paper, we propose the first study to detect non-optimal decisions in ADSs, which lacks the oracles to verify the optimality of the generated paths. To address this issue, we propose a metamorphic testing method, *Decictor*, incorporating a specifically designed

metamorphic relation (MR). *Decictor* comprises three main components: Non-invasive mutation, which generates new scenarios satisfying the constraints described in the MR; MR Check component, verifying whether the scenario's execution adheres to the MR; Feedback-guided selection component, responsible for selecting scenarios for the subsequent mutation. The experimental results demonstrate the effectiveness and efficiency of *Decictor*, as well as the usefulness of each component in *Decictor*.

REFERENCES

- [1] Aldeida Aleti et al. 2022. Identifying Safety-critical Scenarios for Autonomous Vehicles via Key Features. *arXiv preprint arXiv:2212.07566* (2022).
- [2] Matthias Althoff and Sebastian Lutz. 2018. Automatic generation of safety-critical test scenarios for collision avoidance of road vehicles. In *2018 IEEE Intelligent Vehicles Symposium (IV)*. IEEE, Changshu, Suzhou, China, 1326–1333.
- [3] Baidu. 2019. Apollo: Open Source Autonomous Driving. <https://github.com/ApolloAuto/apollo>
- [4] Sai Krishna Bhasetty, Heni Ben Amor, and Georgios Fainekos. 2020. DeepCrashTest: Turning Dashcam Videos into Virtual Crash Tests for Automated Driving Systems. In *2020 IEEE International Conference on Robotics and Automation ICRA*. IEEE, Paris, France, 11353–11360.
- [5] Tsong Yueh Chen, Fei-Ching Kuo, Huai Liu, Pak-Lok Poon, Dave Towey, TH Tse, and Zhi Quan Zhou. 2018. Metamorphic testing: A review of challenges and opportunities. *ACM Computing Surveys (CSUR)* 51, 1 (2018), 1–27.
- [6] Mingfei Cheng, Yuan Zhou, and Xiaofei Xie. 2023. BehAVExplor: Behavior Diversity Guided Testing for Autonomous Driving Systems. In *Proceedings of the 32nd ACM SIGSOFT International Symposium on Software Testing and Analysis*. 488–500.
- [7] comma.ai. 2022. OpenPilot: An open source driver assistance system. Retrieved Nov 7, 2022 from <https://github.com/commaai/openpilot>
- [8] Yao Deng, Xi Zheng, Mengshi Zhang, Guannan Lou, and Tianyi Zhang. 2022. Scenario-based test reduction and prioritization for multi-module autonomous driving systems. In *Proceedings of the 30th ACM Joint European Software Engineering Conference and Symposium on the Foundations of Software Engineering*. 82–93.
- [9] Yao Deng, Xi Zheng, Tianyi Zhang, Huai Liu, Guannan Lou, Miryung Kim, and Tsong Yueh Chen. 2022. A declarative metamorphic testing framework for autonomous driving. *IEEE Transactions on Software Engineering* (2022).
- [10] Shuo Feng, Haowei Sun, Xintao Yan, Haojie Zhu, Zhengxia Zou, Shengyin Shen, and Henry X Liu. 2023. Dense reinforcement learning for safety validation of autonomous vehicles. *Nature* 615, 7953 (2023), 620–627.
- [11] Alessio Gambi, Tri Huynh, and Gordon Fraser. 2019. Generating effective test cases for self-driving cars from police reports. In *Proceedings of the 2019 27th ACM Joint Meeting on European Software Engineering Conference and Symposium on the Foundations of Software Engineering*. ACM, Tallinn Estonia, 257–267.
- [12] Alessio Gambi, Marc Mueller, and Gordon Fraser. 2019. Automatically testing self-driving cars with search-based procedural content generation. In *Proceedings of the 28th ACM SIGSOFT International Symposium on Software Testing and Analysis*. ACM, Beijing, China, 318–328.
- [13] Joshua Garcia, Yang Feng, Junjie Shen, Sumaya Almanee, Yuan Xia, and Qi Alfred Chen. 2020. A comprehensive study of autonomous vehicle bugs. In *Proceedings of the ACM/IEEE 42nd International Conference on Software Engineering*. IEEE, Seoul, South Korea, 385–396.
- [14] Jia Cheng Han and Zhi Quan Zhou. 2020. Metamorphic fuzz testing of autonomous vehicles. In *Proceedings of the IEEE/ACM 42nd International Conference on Software Engineering Workshops*. 380–385.
- [15] Seunghye Han, Jaek Kim, Geon Kim, Jaemin Cho, Jiin Kim, and Shin Yoo. 2021. Preliminary evaluation of path-aware crossover operators for search-based test data generation for autonomous driving. In *2021 IEEE/ACM 14th International Workshop on Search-Based Software Testing (SBST)*. IEEE, Madrid, Spain, 44–47.
- [16] Fitash Ul Haq, Donghwan Shin, and Lionel Briand. 2022. Efficient online testing for DNN-enabled systems using surrogate-assisted and many-objective optimization. In *Proceedings of the 44th International Conference on Software Engineering*. IEEE, Pittsburgh Pennsylvania, 811–822.
- [17] Fitash Ul Haq, Donghwan Shin, and Lionel C Briand. 2023. Many-objective reinforcement learning for online testing of dnn-enabled systems. In *2023 IEEE/ACM 45th International Conference on Software Engineering (ICSE)*. IEEE, 1814–1826.
- [18] Carl Hildebrandt, Meriel von Stein, and Sebastian Elbaum. 2023. PhysCov: Physical Test Coverage for Autonomous Vehicles. In *Proceedings of the 32nd ACM SIGSOFT International Symposium on Software Testing and Analysis*. 449–461.
- [19] Yihan Hu, Jiazhi Yang, Li Chen, Keyu Li, Chonghao Sima, Xizhou Zhu, Siqui Chai, Senyao Du, Tianwei Lin, Wenhai Wang, Lewei Lu, Xiaosong Jia, Qiang Liu, Jifeng Dai, Yu Qiao, and Hongyang Li. 2023. Planning-oriented Autonomous Driving. In *Proceedings of the IEEE/CVF Conference on Computer Vision and Pattern Recognition*.
- [20] Yuqi Huai, Sumaya Almanee, Yuntianyi Chen, Xiafa Wu, Qi Alfred Chen, and Joshua Garcia. 2023. sceno RITA: Generating Diverse, Fully-Mutable, Test Scenarios for Autonomous Vehicle Planning. *IEEE Transactions on Software Engineering* (2023).
- [21] Shinpei Kato, Shota Tokunaga, Yuya Maruyama, Seiya Maeda, Manato Hirabayashi, Yuki Kitsukawa, Abraham Monroy, Tomohito Ando, Yusuke Fujii, and Takuya Azumi. 2018. Autoware on board: Enabling autonomous vehicles with embedded systems. In *2018 ACM/IEEE 9th International Conference on Cyber-Physical Systems (ICCPS)*. IEEE, 287–296.
- [22] LG Electronics. [n. d.]. SVL Simulator Sunset. <https://www.svl simulator.com/news/2022-01-20-svl-simulator-sunset/>.
- [23] Guanpeng Li, Yiran Li, Saurabh Jha, Timothy Tsai, Michael Sullivan, Siva Kumar Sastry Hari, Zbigniew Kalbarczyk, and Ravishankar Iyer. 2020. AV-FUZZER: Finding safety violations in autonomous driving systems. In *2020 IEEE 31st International Symposium on Software Reliability Engineering (ISSRE)*. IEEE, Coimbra, Portugal, 25–36.
- [24] Guannan Lou, Yao Deng, Xi Zheng, Mengshi Zhang, and Tianyi Zhang. 2022. Testing of autonomous driving systems: where are we and where should we go?. In *Proceedings of the 30th ACM Joint European Software Engineering Conference and Symposium on the Foundations of Software Engineering*. 31–43.
- [25] Yixing Luo, Xiao-Yi Zhang, Paolo Arcaini, Zhi Jin, Haiyan Zhao, Fuyuki Ishikawa, Rongxin Wu, and Tao Xie. 2021. Targeting requirements violations of autonomous driving systems by dynamic evolutionary search. In *2021 36th IEEE/ACM International Conference on Automated Software Engineering (ASE)*. IEEE, 279–291.
- [26] Wassim G Najm, Samuel Toma, John Brewer, et al. 2013. *Depiction of priority light-vehicle pre-crash scenarios for safety applications based on vehicle-to-vehicle communications*. Technical Report DOT HS 811 732. National Highway Traffic Safety Administration, U.S. Department of Transportation, Washington, DC.
- [27] Philippe Nitsche, Pete Thomas, Rainer Stuetz, and Ruth Welsh. 2017. Pre-crash scenarios at road junctions: A clustering method for car crash data. *Accident Analysis & Prevention* 107 (2017), 137–151.
- [28] Jan-Pieter Paardekooper, S Montfort, Jeroen Manders, Jorrit Goos, E de Gelder, O Camp, O Bracquemond, and Gildas Thiolon. 2019. Automatic identification of critical scenarios in a public dataset of 6000 km of public-road driving. In *26th International Technical Conference on the Enhanced Safety of Vehicles (ESV)*. Mira Smart, Eindhoven, Netherlands.
- [29] Qi Pang, Yuanyuan Yuan, and Shuai Wang. 2022. MDPFuzz: Testing Models Solving Markov Decision Processes. In *Proceedings of the 31st ACM SIGSOFT International Symposium on Software Testing and Analysis (Virtual, South Korea) (ISSTA 2022)*. Association for Computing Machinery, New York, NY, USA, 378–390. <https://doi.org/10.1145/3533767.3534388>
- [30] Christian Roesener, Felix Fahrenkrog, Axel Uhlig, and Lutz Eckstein. 2016. A scenario-based assessment approach for automated driving by using time series classification of human-driving behaviour. In *2016 IEEE 19th international conference on intelligent transportation systems (ITSC)*. IEEE, Rio de Janeiro, Brazil, 1360–1365.
- [31] Guodong Rong, Byung Hyun Shin, Hadi Tabatabaee, Qiang Lu, Steve Lemke, Märtiņš Možeiko, Eric Boise, Geehoon Uhm, Mark Gerow, Shalin Mehta, et al. 2020. LGSVL simulator: A high fidelity simulator for autonomous driving. In *2020 IEEE 23rd International Conference on Intelligent Transportation Systems (ITSC)*. IEEE, Rhodes, Greece, 1–6.
- [32] Yun Tang, Yuan Zhou, Yang Liu, Jun Sun, and Gang Wang. 2021. Collision avoidance testing for autonomous driving systems on complete maps. In *2021 IEEE Intelligent Vehicles Symposium (IV)*. IEEE, Nagoya, Japan, 179–185.
- [33] Yun Tang, Yuan Zhou, Fenghua Wu, Yang Liu, Jun Sun, Wuling Huang, and Gang Wang. 2021. Route coverage testing for autonomous vehicles via map modeling. In *2021 IEEE International Conference on Robotics and Automation (ICRA)*. IEEE, Xi'an, China, 11450–11456.
- [34] Yun Tang, Yuan Zhou, Tianwei Zhang, Fenghua Wu, Yang Liu, and Gang Wang. 2021. Systematic testing of autonomous driving systems using map topology-based scenario classification. In *Proceedings of the 36th IEEE/ACM International Conference on Automated Software Engineering (ASE)*. IEEE, Melbourne, Australia, 1342–1346.
- [35] Eric Thorn, Shawn C Kimmel, Michelle Chaka, Booz Allen Hamilton, et al. 2018. *A framework for automated driving system testable cases and scenarios*. Technical Report. United States. Department of Transportation. National Highway Traffic Safety.
- [36] Shuai Wang and Zhendong Su. 2021. Metamorphic object insertion for testing object detection systems. In *Proceedings of the 35th IEEE/ACM International Conference on Automated Software Engineering (Virtual Event, Australia)*. Association for Computing Machinery, New York, NY, USA, 1053–1065.
- [37] Xiaoyuan Xie, Ying Duan, Songqiang Chen, and Jifeng Xuan. 2022. Towards the Robustness of Multiple Object Tracking Systems. In *2022 IEEE 33rd International Symposium on Software Reliability Engineering (ISSRE)*. IEEE, 402–413.
- [38] Xiaoyuan Xie, Joshua WK Ho, Christian Murphy, Gail Kaiser, Baowen Xu, and Tsong Yueh Chen. 2011. Testing and validating machine learning classifiers by metamorphic testing. *Journal of Systems and Software* 84, 4 (2011), 544–558.

- [39] Mengshi Zhang, Yuqun Zhang, Lingming Zhang, Cong Liu, and Sarfraz Khurshid. 2018. DeepRoad: GAN-based metamorphic testing and input validation framework for autonomous driving systems. In *Proceedings of the 33rd ACM/IEEE International Conference on Automated Software Engineering*. 132–142.
- [40] Xudong Zhang and Yan Cai. 2023. Building Critical Testing Scenarios for Autonomous Driving from Real Accidents. In *Proceedings of the 32nd ACM SIGSOFT International Symposium on Software Testing and Analysis*. 462–474.
- [41] Zhejun Zhang, Alexander Liniger, Dengxin Dai, Fisher Yu, and Luc Van Gool. 2021. End-to-end urban driving by imitating a reinforcement learning coach. In *Proceedings of the IEEE/CVF international conference on computer vision*. 15222–15232.
- [42] Ziyuan Zhong, Gail Kaiser, and Baishakhi Ray. 2023. Neural network guided evolutionary fuzzing for finding traffic violations of autonomous vehicles. *IEEE Transactions on Software Engineering* 49, 4 (2023), 1860–1875.
- [43] Yuan Zhou, Yang Sun, Yun Tang, Yuqi Chen, Jun Sun, Christopher M Poskitt, Yang Liu, and Zijiang Yang. 2023. Specification-based Autonomous Driving System Testing. *IEEE Transactions on Software Engineering* (2023), 1–19.
- [44] Zhi Quan Zhou and Liqun Sun. 2019. Metamorphic testing of driverless cars. *Commun. ACM* 62, 3 (2019), 61–67.